Optik 124 (2013) 5866–5870

Contents lists available at ScienceDirect

Optik

journal homepage: www.elsevier.de/ijleo

Advantage of InGaN-based light-emitting diodes using AlGaInN electron blocking layer coupled with inserting InGaN layer

Tian-Hu Wang[a], Jin-Liang Xu[b,*]

[a] Beijing Key Laboratory of New and Renewable Energy, North China Electric Power University, Beijing 102206, China
[b] Beijing Key Laboratory of Multiphase Flow and Heat Transfer, North China Electric Power University, Beijing 102206, China

ARTICLE INFO

Article history:
Received 19 November 2012
Accepted 16 April 2013

Keywords:
Light-emitting diodes
Efficiency droop
Electron blocking layer
InGaN

ABSTRACT

In this paper, we demonstrate the improved performance of light-emitting diodes (LED) with AlGaInN electron blocking layer (EBL) by inserting a p-type InGaN layer in front of it. The performances of three LED structures with conventional AlGaN EBL, AlGaInN EBL and AlGaInN EBL coupled with an inserted p-type InGaN layer are numerically studied. The output power performance is significantly improved and the efficiency droop could reduce to only 4% when a p-type InGaN layer was inserted in front of the AlGaInN EBL, which is responsible for the reduced electron leakage and enhanced hole injection efficiency, as well as alleviated electrostatic fields in the quantum wells.

1. Introduction

The III-nitride based light-emitting diodes have attracted much attention due to their energy saving, compact size and long lifetime. Thus, they are widely used in solid-state illumination, back-lighting, full-color display, etc. [1,2]. The internal quantum efficiency (IQE) of InGaN LEDs reaches its peak value at low injection current and then decreases gradually with further increases of injection currents, which is well known as the efficiency droop [2,3]. This phenomenon leads to great restriction to developing high power solid state lighting. Several mechanisms of the efficiency droop have been explored in the past few years. Among these studies, the polarization effect arising from the surface charges at hetero interfaces in GaN-based materials [3,4] has a significant effect on the LED performance, which is against the optical and electrical properties and is responsible for the efficiency droop in three ways: (1) due to the surface charges at the well/barrier interfaces, the polarization-induced electric field modifies the energy band to form triangular wells in multiple quantum wells (MQWs), separating the electron and hole wave functions in multi-quantum wells to severely reduce the radiative efficiency. This phenomenon is called the quantum confined Stark effect (QCSE) [5–7]; (2) the polarization effect lowers the energy band at the last-barrier/EBL interface, reducing the effective potential barrier height for electron of the AlGaN EBL [3,4,8,9]; (3) the downward band-bending at the last-barrier/EBL interface forms an obstacle barrier for the holes injection into the active region [9–11].

To improve the droop efficiency effect, several methods, such as the polarization reduced barriers [4–6], staggered QWs [7], AlInN EBL [8], graded EBL [9,11], n-type AlGaN EBL [12], removing the EBL [13], and thin last barrier structure [14], have been proposed. Even though the AlGaInN EBL can effectively reduce the efficiency droop [3,5], considerable electron leakage [3] still exists. In this paper, we further improve the LED performance by inserting a p-type InGaN layer in front of the AlGaInN EBL. This novel design not only enhances the electron confinement and hole injection efficiency, but also reduces the QCSE in the MQWs.

2. Device structure and parameters

The LED A used as the reference structure was prepared on a c-plane sapphire substrate. Before the growth of InGaN/GaN MQWs, a 50-nm-thick un-doped GaN buffer layer was deposited and then a 2.95-μm-thick Si-doped n-type GaN layer was grown (n-doping = 5×10^{18} cm^{-3}). The active region consists of five 2.5-nm-thick $In_{0.15}Ga_{0.85}N$ quantum wells, separated by six 9-nm-thick GaN barriers. On the top of the active region were a 20-nm-thick p-type $Al_{0.15}Ga_{0.85}N$ EBL (p-doping = 5×10^{17} cm^{-3}) and a 150-nm-thick p-type GaN cap layer (p-doping = 1.2×10^{18} cm^{-3}). The device geometry was 300×300 μm^2. The LED B is identical to LED A except that the AlGaN EBL was replaced by a p-type $Al_{0.38}Ga_{0.46}In_{0.16}N$ EBL (p-doping = 5×10^{17} cm^{-3}). The LED C is identical to LED B except that a 10-nm-thick p-type $In_{0.1}Ga_{0.9}N$ layer (p-doping = 1.2×10^{18} cm^{-3}) was inserted between the last

* Corresponding author. Tel.: +86 10 61772268; fax: +86 10 61772268.
E-mail address: xjl@ncepu.edu.cn (J.-L. Xu).

0030-4026/$ – see front matter © 2013 Elsevier GmbH. All rights reserved.
http://dx.doi.org/10.1016/j.ijleo.2013.04.065

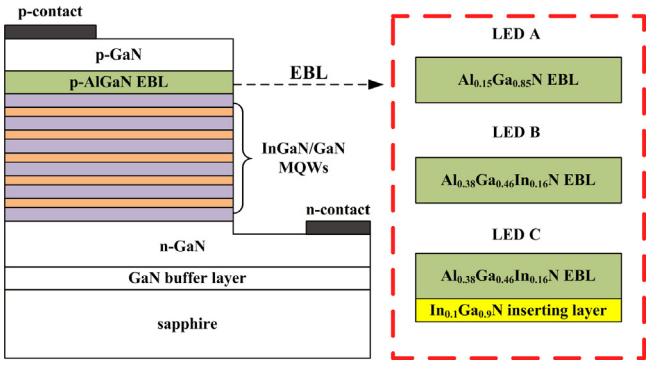

Fig. 1. The schematic diagrams for LEDs A, B and C.

Table 1
Material parameters used in the simulation for the binary semiconductor compound energy band gaps.

Parameters	InN	GaN	AlN
$E_g(0)$ (eV)	0.735	3.507	6.23
α (meV/K)	0.245	0.909	1.799
β (K)	624	830	1462

GaN barrier and the $Al_{0.38}Ga_{0.46}In_{0.16}N$ EBL. Fig. 1 shows the schematic diagrams of the three LED structures.

The LED optical and electrical properties were numerically investigated with the APSYS simulation program [15] (Crosslight Software Inc.), which solves Poisson's equation, current continuity equations, carrier transport equation, quantum mechanical wave equation and photon rate equation. The non-radiative recombination processes and current leakage are taken into account. The Shockley–Read–Hall (SRH) recombination lifetime, radiative and Auger recombination coefficients are 100 ns, 2×10^{-11} cm^3 s^{-1}, and 1×10^{-34} cm^6 s^{-1}, respectively. The band offset ratio is assumed to be 0.7:0.3 which is similar to the reported values by Piprek and Nakamura [16]. The internal absorption within the LED device and the light extraction efficiency are assumed to 500 m^{-1} and 78%, respectively.

APSYS employs the 6×6 $k{\cdot}p$ model to calculate the energy band structures, which was developed by Chuang and Chang [17,18]. The band gap energy of InN, GaN, and AlN as a function of temperature T can be expressed by the Varshni formula [19]:

$$E_g(T) = E_g(0) - \frac{\alpha \cdot T^2}{T + \beta}, \tag{1}$$

where $E_g(T)$ is the band gap energy at temperature T, $E_g(0)$ is the band gap energy at 0 K, α and β are material related constants. The values of $E_g(0)$, α, and β for InN, GaN, and AlN are listed in Table 1. The temperature is set to be 300 K in the simulation. For ternary alloys of InGaN and AlGaN, the band gap energies can be expressed as follows [19]:

$$E_g(In_xGa_{1-x}N) = E_g(InN) \cdot x + E_g(GaN) \cdot (1-x) - b(InGaN) \cdot x \cdot (1-x), \tag{2}$$

$$E_g(Al_xGa_{1-x}N) = E_g(AlN) \cdot x + E_g(GaN) \cdot (1-x) - b(AlGaN) \cdot x \cdot (1-x), \tag{3}$$

where $E_g(In_xGa_{1-x}N)$ and $E_g(Al_xGa_{1-x}N)$ are the band gap energies of $In_xGa_{1-x}N$ and $Al_xGa_{1-x}N$, the bowing parameters for InGaN and AlGaN are 1.43 eV and 1.0 eV, respectively. The energy band gap of $Al_xGa_{1-x-y}In_yN$ can be expressed as the following formulas:

$$E_g(Al_xGa_{1-x-y}In_yN) = \frac{xyE_g(AlInN) + yzE_g(InGaN) + xzE_g(AlGaN)}{xy + yz + zx}, \tag{4}$$

$$E_g(AlInN) = uE_g(InN) + (1-u)E_g(AlN) - u(1-u)b(AlInN), \tag{5}$$

$$E_g(InGaN) = vE_g(GaN) + (1-v)E_g(InN) - v(1-v)b(InGaN), \tag{6}$$

$$E_g(AlGaN) = wE_g(GaN) + (1-w)E_g(AlN) - w(1-w)b(AlGaN), \tag{7}$$

$$u = \frac{1-x+y}{2}, \quad v = \frac{1-y+x}{2}, \quad w = \frac{1-x+z}{2}, \tag{8}$$

where x, y and $z = 1 - x - y$ are the compositions of Al, In and Ga in the AlGaInN material, respectively. The band bowing parameter for $Al_xIn_{1-x}N$ is 2.5 eV. Other material parameters of the semiconductors used in the simulation can be found in Ref. [20].

The charge density induced by the spontaneous and piezoelectric polarization at the hetero interface can be calculated by the method developed by Fiorentini et al. [21]. The spontaneous polarization (C/m^2) of the ternary nitride alloys and AlGaInN alloy can be expressed as:

$$P_{sp}(In_xGa_{1-x}N) = -0.042 \cdot x - 0.034 \cdot (1-x) + 0.037 \cdot x \cdot (1-x), \tag{9}$$

$$P_{sp}(Al_xGa_{1-x}N) = -0.090 \cdot x - 0.034 \cdot (1-x) + 0.019 \cdot x \cdot (1-x), \tag{10}$$

$$P_{sp}(Al_xGa_{1-x-y}In_yN) = -0.090 \cdot x - 0.042 \cdot y - 0.034 \cdot (1-x-y) + 0.07 \cdot xy + 0.037 \cdot y \cdot (1-x-y) + 0.021 \cdot x \cdot (1-x-y). \tag{11}$$

The piezoelectric polarization (C/m^2) of ternary alloys and AlGaInN alloy can be expressed as:

$$P_{pz}(In_xGa_{1-x}N) = P_{pz}(InN) \cdot x + P_{pz}(GaN) \cdot (1-x), \tag{12}$$

$$P_{pz}(Al_xGa_{1-x}N) = P_{pz}(AlN) \cdot x + P_{pz}(GaN) \cdot (1-x), \tag{13}$$

$$P_{pz}(Al_xGa_{1-x-y}In_yN) = P_{pz}(AlN) \cdot x + P_{pz}(InN) \cdot y + P_{pz}(GaN) \cdot (1-x-y), \tag{14}$$

where

$$P_{pz}(InN) = -1.373 \cdot \varepsilon + 7.559 \cdot \varepsilon^2, \tag{15}$$

$$P_{pz}(GaN) = -0.918 \cdot \varepsilon + 9.541 \cdot \varepsilon^2, \tag{16}$$

$$P_{pz}(AlN) = -1.808 \cdot \varepsilon + 5.642 \cdot \varepsilon^2 \quad (\varepsilon < 0), \tag{17}$$

$$P_{pz}(AlN) = -1.808 \cdot \varepsilon - 7.888 \cdot \varepsilon^2 \quad (\varepsilon > 0). \tag{18}$$

The basal strain for the alloy matched to the GaN layer is defined as:

$$\varepsilon = \frac{(a_{sub} - a)}{a}, \tag{19}$$

where a_{sub} and a are the lattice constants of the GaN and alloy layers, respectively. The total polarization is the sum of the spontaneous and piezoelectric polarization. Considering the screening caused by defects, the surface charge densities are generally varied from 20% to 80% as compared to that of theoretical calculations [22,23]. In this study, the interface charge density is assumed to be 50% of the calculated values.

Table 2
Material parameters used in the simulation for carrier mobility.

Parameters	AlGaN	InGaN
$\mu_{max,n}$ ($cm^2\,V^{-1}\,s^{-1}$)	306	684
$\mu_{min,n}$ ($cm^2\,V^{-1}\,s^{-1}$)	132	386
$N_{ref,n}$ (cm^{-3})	1×10^{17}	1×10^{17}
α_n	0.29	1.37
$\mu_{max,p}$ ($cm^2\,V^{-1}\,s^{-1}$)	10	2
$\mu_{min,p}$ ($cm^2\,V^{-1}\,s^{-1}$)	10	2
$N_{ref,p}$ (cm^{-3})	3×10^{17}	2.75×10^{17}
α_p	0.395	0.395

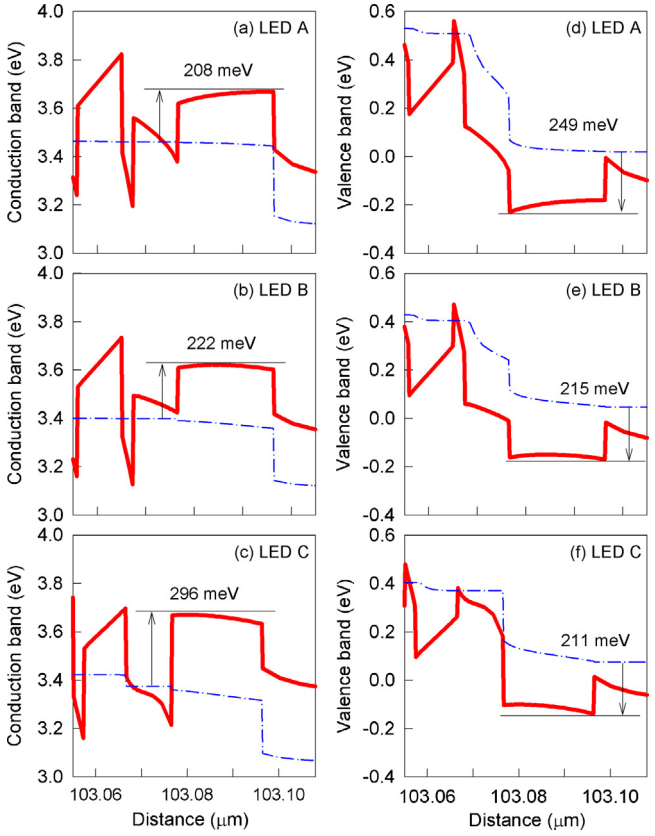

Fig. 2. Energy band diagrams near the electron blocking layer for the three LEDs at 150 mA. (a)–(c) conduction band; (d)–(f) valence band.

The Caughey–Thomas approximation [24] is employed in the simulation for the carrier mobility as a function of carrier density which can be expressed as follows:

$$\mu_i(N) = \mu_{\min,i} + \frac{\mu_{\max,i} - \mu_{\min,i}}{1.0 + (N/N_{ref,i})^{\alpha,i}}, \tag{20}$$

where i denotes either electron or hole, all parameters in the formula are listed in Table 2.

3. Analysis and discussion

Fig. 2 shows the energy band diagrams and quasi-Fermi levels near the EBL and last-barrier of the LEDs A, B and C at 150 mA. A sloped triangular barrier and band downward bending induced by the polarization effect [3,4] at the last-barrier/EBL interface were observed in LED A, causing serious electron leakage and poor hole injection. It is apparent that there exists a low energy point at which the conduction band energy is below the quasi-Fermi level at the last-barrier/EBL interface. When the AlGaInN EBL was used, the band-bending phenomenon was improved and the low energy

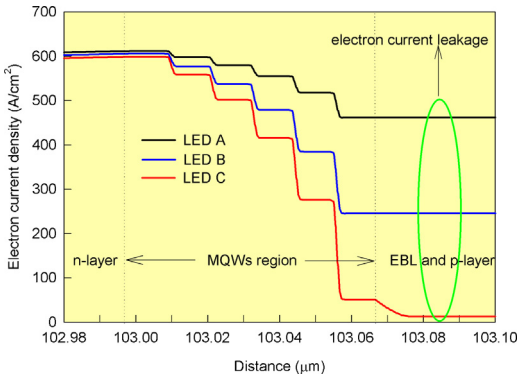

Fig. 3. Electron current leakage profiles near the active region for the three LEDs at 150 mA.

point has been lifted to be above the quasi-Fermi level due to the improved lattice match [5]. For the conduction band of LED C, as indicated in Fig. 2(c), inserting InGaN layer produces a deep triangle potential well in front of the EBL, which can confine more electron from overflowing to the p-type layer and decease the electron leakage dramatically. As indicated in Fig. 2(a)–(c), the effective potential barrier heights of the EBLs for LEDs A, B and C are 208 meV, 222 meV and 296 meV, respectively. It is apparent that the effective barrier for confining electron in LED C is substantially enhanced.

Moreover, in the valence band of LED C, the downward band bending sloped upward from left side to right side of the EBL is level down and even overturn compared to those of LEDs A and B. This results in the reduced obstacle barrier potential height for holes than those of LED A (i.e. from 249 meV to 211 meV) and LED B (i.e. from 215 meV to 211 meV), which improve the efficiency of hole injection. Consequently, when a p-type InGaN layer was inserted between the last GaN barrier and the AlGaInN EBL, the relatively lower band gap energy of InGaN layer can not only increase the effective potential barrier height of the conduction band but also decrease the obstacle barrier height for hole injection in the valence band. According to this proper modified energy band diagram, the diminished electron overflow and enhance hole injection efficiency can be expected. This could be justified by the vertical electron current leakage profiles of the three LEDs.

Fig. 3 plots the vertical electron current density distribution near the active region for the three LEDs at 150 mA. As expected, the electron current leakage in LED A is the most serious of the three LEDs, due to the poor hole injection efficiency and significant electron spillover effect induced by the downward band bending. When the EBL is replaced by an AlGaInN one, the leakage effect is alleviated as the reason that the electron blocking effect is enhanced and the situation retarding holes injecting from p-layer to the active region is improved by the less polarization sheet charges at the hetero interface. What is more, the electron leakage could be further suppressed by inserting an InGaN layer between the last GaN layer and the EBL, which dramatically keep more electrons in the active region to recombine with holes. When the leaked elections to the p-layer are diminished, the hole injection efficiency into the active region could be lifted up because the holes recombined with leaked electrons non-radiatively outside the MQWs are decreased and more holes can reach the active region. Thus, both the electron and hole concentrations in the active region will increase.

Fig. 4 shows the carrier concentration in the active region for the three LEDs as 150 mA. It is apparent that both the concentrations of electron and hole in the active region for LED C are obvious increased compared to LEDs A and B, which demonstrates the improved efficiency of electron confinement and hole injection.

Fig. 5 shows the electrostatic fields in the every QW for the three LEDs at 150 mA. The large electrostatic field in the MQWs

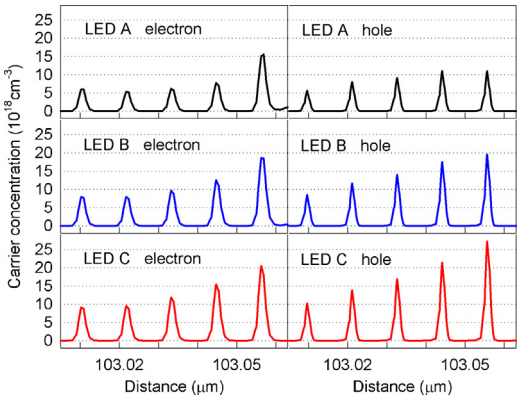

Fig. 4. Carrier concentrations in the active region for the three LEDs at 150 mA.

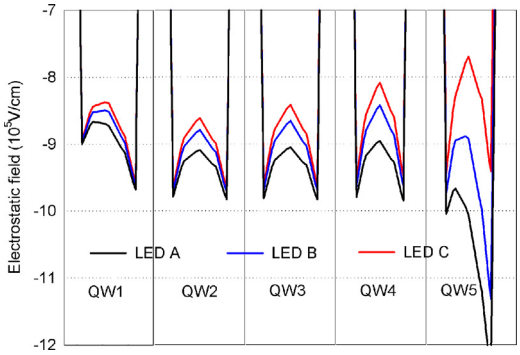

Fig. 5. Electrostatic fields in the five quantum wells for the three LEDs at 150 mA.

region results in quantum confined Stark effect and poor overlap of hole and electron wave functions. As a result, it reduces the radiative recombination rate and internal quantum efficiency [25,26]. In addition to the enhanced carrier concentration in the active region, the electrostatic fields in the MQWs are also decreased by inserting InGaN layer, which means that the overlap of electron–hole wave function and radiative recombination efficiency could be enhanced. Consequently, the optical performance can benefit from both the increased carrier concentration and reduced QCSE in the MQWs. This can be verified by the radiative recombination rate in the active region as shown in Fig. 6. Fig. 6 shows the radiative recombination rates for LEDs A, B and C in the active region at 150 mA, respectively. It is evident that, the radiative recombination rates are enhanced in every QW for LED C. In details, the rate is increased by a factor

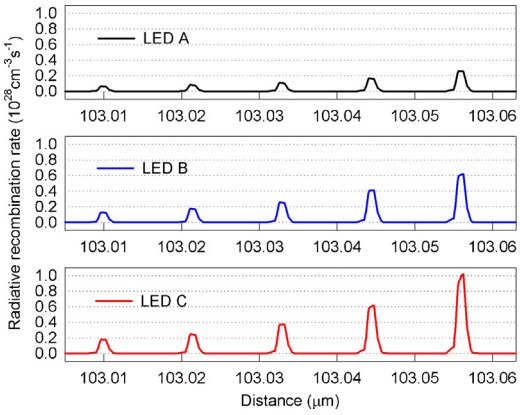

Fig. 6. Radiative recombination rates in the active region for the three LEDs at 150 mA.

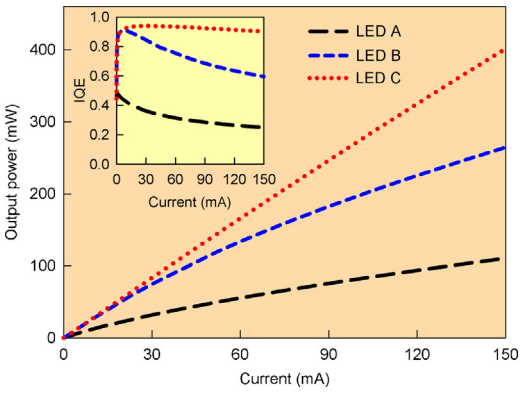

Fig. 7. Output power and internal quantum efficiency as a function of injection current of the three LEDs.

of 3.5 and 1.5 for LED C compared to those of LEDs A and LED B, respectively

Fig. 7 shows the light output power and IQE (inserted figure) performance curves for LEDs A, B and C under study as a function of injection current. The efficiency droops, which are defined as the formula $(IQE_{peak} - IQE_{min})/IQE_{peak}$, are 50% and 34% for LEDs A and B, respectively. As for LED C specially, The IQE still keeps the value of 0.94 at 150 mA and its efficiency droop reduce to only 4%. The enhanced IQE leads to the improved output power. The LED A with AlGaN EBL shows the lowest output power at high current. As the AlGaInN EBL was used, the performance of output power is improved. Due to the above-mentioned advantage of LED C, it exhibits the best output power characteristics among the three LEDs, which is superior to LED A and LED B by improved ratios of 1.5 and 3.7 for output power at 150 mA, respectively. As a result, LED C is the best one to work under high injection current due to its smallest efficiency droop.

4. Conclusion

In summary, advantage of light-emitting diodes with AlGaInN electron blocking layer coupled by inserting InGaN layer was proposed and numerical studied. The energy band diagrams, carrier concentration, electron leakage current, radiative recombination rates, electrostatic fields in the active region and efficiency droop are systematically investigated and compared among the proposed LED C and other two reference LEDs A and B. The results suggest that the performance of the LED with AlGaInN EBL could be further enhanced due to the enhanced electron confinement, increased hole injection efficiency and reduced electrostatic fields in the active region by inserting an InGaN layer in front of the AlGaInN EBL. The results also show that efficiency droop can be reduced to only 4% of the proposed structure LED C, thus, it is the best choice to be used at high injection currents.

Acknowledgements

This work was financially supported by the National Natural Science Foundation of China (U1034004, 50825603 and 51210011), and the Fundamental Research Funds for the Central Universities (12QX14).

References

[1] M.R. Krames, O.B. Shchekin, R. Mueller-Mach, G.O. Mueller, L. Zhou, G. Harbers, M.G. Craford, Status and future of high-power light-emitting diodes for solid-state lighting, IEEE J. Display Technol. 3 (2007) 160–175.

[2] S. Singh, N.K. Rohila, S. Pal, C. Dhanavantri, Optimization towards reduction of efficiency droop in blue GaN/InGaN based light emitting diodes, Optik 123 (2012) 1287–1292.
[3] M.H. Kim, M.F. Schubert, Q. Dai, J.K. Kim, E.F. Schubert, J. Piprek, Y. Park, Origin of efficiency droop in GaN-based light-emitting diodes, Appl. Phys. Lett. 91 (2007) 183507.
[4] M.F. Schubert, J. Xu, J.K. Kim, E.F. Schubert, M.H. Kim, S. Yoon, S.M. Lee, C. Sone, T. Sakong, Y. Park, Polarization-matched GaInN/AlGaInN multi-quantum-well light-emitting diodes with reduced efficiency droop, Appl. Phys. Lett. 93 (2008) 041102.
[5] Y.K. Kuo, M.C. Tsai, S.H. Yen, Numerical simulation of blue InGaN light-emitting diodes with polarization-matched AlGaInN electron-blocking layer and barrier layer, Opt. Commun. 282 (2009) 4252–4255.
[6] Y.K. Kuo, J.Y. Chang, M.C. Tsai, S.H. Yen, Advantages of blue InGaN multiple-quantum well light-emitting diodes with InGaN barriers, Appl. Phys. Lett. 95 (2009) 011116.
[7] C.T. Liao, M.C. Tsai, B.T. Liou, S.H. Yen, Y.K. Kuo, Improvement in output power of a 460 nm InGaN light-emitting diode using staggered quantum well, J. Appl. Phys. 108 (2010) 063107.
[8] S. Choi, H.J. Kim, S.S. Kim, J. Liu, J. Kim, J.H. Ryou, R.D. Dupuis, A.M. Fischer, F.A. Ponce, Improvement of peak quantum efficiency and efficiency droop in III-nitride visible light-emitting diodes with an InAlN electron-blocking layer, Appl. Phys. Lett. 96 (2010) 221105.
[9] C.H. Wang, C.C. Ke, C.Y. Lee, S.P. Chang, W.T. Chang, J.C. Li, Z.Y. Li, H.C. Yang, H.C. Kuo, T.C. Lu, S.C. Wang, Hole injection and efficiency droop improvement in InGaN/GaN light-emitting diodes by band-engineered electron blocking layer, Appl. Phys. Lett. 97 (2010) 261103.
[10] S.H. Han, D.Y. Lee, S.J. Lee, C.Y. Cho, M.K. Kwon, S.P. Lee, D.Y. Noh, D.J. Kim, Y.C. Kim, S.J. Park, Effect of electron blocking layer on efficiency droop in InGaN/GaN multiple quantum well light-emitting diodes, Appl. Phys. Lett. 94 (2009) 231123.
[11] Y.K. Kuo, J.Y. Chang, M.C. Tsai, Enhancement in hole injection efficiency of blue InGaN light-emitting diodes from reduced polarization by some specific designs on electron blocking layer, Opt. Lett. 35 (2010) 3285–3287.
[12] S.H. Yen, M.C. Tsai, M.L. Tsai, Y.J. Shen, T.C. Hsu, Y.K. Kuo, Effect of n-type AlGaN layer on carrier transportation and efficiency droop of blue InGaN light-emitting diodes, IEEE Photon. Technol. Lett. 21 (2009) 975–977.
[13] H.Y. Ryu, J.-I. Shim, C.-H. Kim, J.H. Choi, H.M. Jung, M.S. Noh, J.M. Lee, E.S. Nam, Efficiency and electron leakage characteristics in GaN-based light-emitting diodes without AlGaN electron blocking layer structures, IEEE Photon. Technol. Lett. 23 (2011) 1866–1868.
[14] S.H. Yen, M.L. Tsai, M.C. Tsai, S.J. Chang, Y.K. Kuo, Investigation of optical performance of InGaN MQW LED with thin last barrier, IEEE Photon. Technol. Lett. 22 (2010) 1787–1789.
[15] APSYS by Crosslight Software Inc., Burnaby, Canada.
[16] J. Piprek, S. Nakamura, Physics of high-power InGaN/GaN lasers, Inst. Electr. Eng. Proc. Optoelectron. 149 (2002) 145–151.
[17] S.L. Chuang, C.S. Chang, $k\cdot p$ method for strained wurtzite semiconductors, Phys. Rev. B 54 (1996) 2491–2504.
[18] S.L. Chuang, C.S. Chang, A band-structure model of strained quantum-well wurtzite semiconductors, Semicond. Sci. Technol. 12 (1997) 252–263.
[19] I. Vurgaftman, J.R. Meyer, L.R. Ram-Mohan, Band parameters for III–V compound semiconductors and their alloys, J. Appl. Phys. 89 (2001) 5815–5875.
[20] I. Vurgaftman, J.R. Meyer, Band parameters for nitrogen containing semiconductors, J. Appl. Phys. 94 (2003) 3675–3696.
[21] V. Fiorentini, F. Bernardini, O. Ambacher, Evidence for nonlinear macroscopic polarization in III-V nitride alloy heterostructures, Appl. Phys. Lett. 80 (2002) 1204–1206.
[22] F. Renner, P. Kiesel, G.H. Döhler, M. Kneissl, C.G. Van de Walle, N.M. Johnson, Quantitative analysis of the polarization fields and absorption changes in InGaN/GaN quantum wells with electroabsorption spectroscopy, Appl. Phys. Lett. 81 (2002) 490–492.
[23] H. Zhang, E.J. Miller, E.T. Yu, C. Poblenz, J.S. Speck, Measurement of polarization charge and conduction-band offset at $In_xGa_{1-x}N$/GaN heterojunction interfaces, Appl. Phys. Lett. 84 (2004) 4644–4646.
[24] C.M. Caughey, R.E. Thomas, Carrier mobilities in silicon empirically related to doping and field, Proc. IEEE 55 (1967) 2192–2193.
[25] S.H. Park, S.L. Chuang, Piezoelectric effects on electrical and optical properties of wurtzite GaN/AlGaN quantum well lasers, Appl. Phys. Lett. 72 (1998) 3103–3105.
[26] H.P. Zhao, G.Y. Liu, J. Zhang, J.D. Poplawsky, V. Dierolf, N. Tansu, Approaches for high internal quantum efficiency green InGaN light-emitting diodes with large overlap quantum wells, Opt. Express 19 (2011) A991–A1007.